



# ARCHIVES of FOUNDRY ENGINEERING

ISSN (2299-2944)  
Volume 2022  
Issue 2/2022

50 – 56

10.24425/afe.2022.140224

5/2

Published quarterly as the organ of the Foundry Commission of the Polish Academy of Sciences

## Initial Analysis of the Surface Layer of AVGI Cast Iron Subject to Abrasion

A. Jakubus 

The Jacob of Paradies University in Gorzów Wielkopolski, ul. Teatralna 25, 66-400 Gorzów Wielkopolski, Poland

\* Corresponding author. E-mail address: jakubusaneta@wp.pl

Received 10.12.2021; accepted in revised form 15.03.2022; available online 16.05.2022

### Abstract

The article presents the results of research on the abrasion resistance of cast iron with vermicular graphite in the as-cast state and after austempering (the latter material is referred to as AVGI – Austempered Vermicular Graphite Iron). Austenitization was carried out at the temperature values of either 900°C or 960°C, and austempering at the temperature values of either 290°C and or 390°C. Both the austenitization and the austempering time was equal to 90 minutes. The change of the pearlitic-ferritic matrix to the ausferritic one resulted in an increase in mechanical properties. Abrasion tests were conducted by means of the T-01M pin-on-disc tribometer. The counter-sample (i.e. the disc) was made of the JT6500 friction material. Each sample was subject to abrasion over a sliding distance of 4000 m. The weight losses of both samples and counter-samples were determined by the gravimetric method. It was found that the vermicular cast iron austenitized at 900°C and austempered at 290°C was characterized by the lowest wear among the evaluated cast iron types. The geometric structure of the surface layer after the dry friction test exhibited irregular noticeable grooves, distinct oriented abrasion traces, plastic flow of the material, microcracks, and pits generated by tearing out the abraded material. The largest surface roughness was found for the AVGI cast iron heat-treated according to the variant 3 ( $T_{\gamma}=900^{\circ}\text{C}$ ;  $T_{pi}=390^{\circ}\text{C}$ ), while the smallest one occurred in AVGI cast iron subject to either the variant 2 ( $T_{\gamma}=960^{\circ}\text{C}$ ;  $T_{pi}=290^{\circ}\text{C}$ ) or the variant 4 ( $T_{\gamma}=900^{\circ}\text{C}$ ;  $T_{pi}=290^{\circ}\text{C}$ ) of heat treatment and was equal to either 2.5  $\mu\text{m}$  or 2.66  $\mu\text{m}$ , respectively. It can be seen that the surface roughness decreases with the decrease in the austempering temperature.

**Keywords:** Vermicular cast iron, Abrasion resistance, Austempering, Abrasion of cast iron, AVGI

### 1. Introduction

All tribological processes taking place in the elements of various machines and devices occur in the surface layers of the friction elements. The effect of friction is the wear of machine elements, which causes changes in surface geometry, changes of shape, as well as accumulation of macro- and micro-defects resulting in decohesion of the surface layer material [1]. The operational strength of sliding elements is mainly determined by both the surface and the volume strength of their top layers [2].

Elements of machines and devices of the required high abrasion resistance are made of either white or grey cast iron [3; 4], as well as of steel (in this case their tribological properties

can be increased e.g. by creating an alloyed surface layer [5]). Such parts as clutches, shoes, brake drums and rollers work under the dry friction conditions. Considerable stresses and high temperature values are generated during sliding or rolling of the cooperating elements of machines and devices. The occurrence of these problems entails the need to increase thermal conductivity, ensure dimensional stability and stop physical transformations within the range of working temperature of the cooperating elements. It should be noted that grey cast iron shows a very good thermal conductivity and the ability to dampen vibrations. The latter properties are slightly worse in the case of the vermicular graphite cast iron, but the material exhibits better strength and plastic properties. Many researchers analyse also the abrasion of ductile iron [e.g. 6-10], which strength is much higher as



compared with grey cast iron, but the material tends to warp due to, inter alia, its low thermal conductivity. The change in structure from the ductile iron to the austempered ductile iron (ADI), results in the improvement of selected functional properties, e.g. the abrasion resistance [11-18].

The as-cast vermicular graphite cast iron exhibits good abrasion resistance, high resistance to mechanical stresses, fast heat dissipation, as well as high strength and hardness. This set of properties stimulates the highly industrialised countries to use this material in the production of brake discs for cars and railway equipment, as well as camshafts, or other parts of machines resistant to abrasion and subject to intensive stress [19]. Exposing the vermicular cast iron to austempering with the isothermal transformation can increase the scope of application of the material, as the appropriate selection of heat treatment parameters may significantly affect both the strength and the abrasion resistance of the material.

Austempering of steel results in the formation of microstructure consisting of the acicular ferrite and iron carbide (cementite), but in the case of the austempered cast iron the microstructure consists of the high-carbon austenite and acicular ferrite [20-26]. It should be noted that not only the basic elements present in cast iron, but also certain alloying elements significantly influence the heat treatment process. For example, the hardenability of cast iron decreases with increasing carbon and silicon content, and increases with increasing manganese, copper, nickel, chromium and molybdenum content. It is also important that as the austenitization temperature increases, the fraction of high-carbon austenite at the end of the first stage of isothermal transformation of austenite increases [3].

## 2. The purpose of investigation and the research material

The aim of the research was the analysis of the surface layer of vermicular graphite cast iron under the conditions of abrasive wear, both for the as-cast and for the heat-treated material.

Specimens for examination were cut out of the U-shaped test blocks of the IIb type [27] with the wall thickness equal to 25mm. Chemical composition of the examined vermicular graphite cast iron is presented in Table 1. Figure 1 shows the microstructure of the alloy in question in the as-cast state.

Table 1.

Chemical compositions of vermicular graphite cast iron

Content of elements, wt.%						
C	Si	Mn	Cu	P	S	Mg
3.22	2.38	0.192	1.02	0.054	0.022	0.027

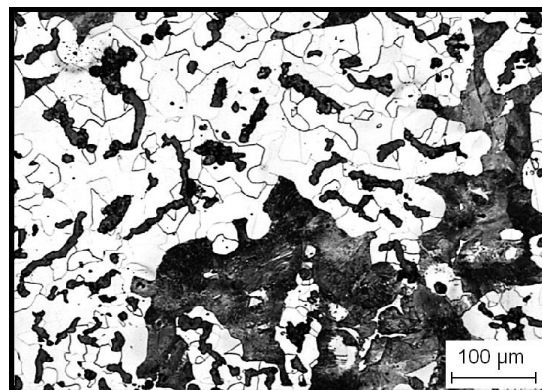


Fig. 1. The microstructure of vermicular graphite cast iron in the as-cast state; etched with 2% Nital etchant

The examined vermicular cast iron in the as-cast state contained over 95% of vermicular graphite precipitates, and about 5% of nodular graphite (according to the standard [28]). The alloy was characterized by the pearlitic-ferritic matrix and the percentage of each of these two phases was approximately 50% (according to the standard [29]). It is worth noting that even the copper content exceeding one percent did not ensure the occurrence of the fully pearlitic matrix in this alloy. This happened due to the specific crystallization course of the examined alloy and to its tendency to form the ferritic matrix.

The heat treatment was carried out in Odlewnie Polskie S.A. enterprise in Starachowice. The austenitization process was held in an air atmosphere by means of the resistance chamber furnace made by Elterma S.A. Company. Austempering was performed in a quenching tank, the salt bath being used as the quenching agent. Cylindrical specimens, 20 mm in diameter and 160 mm in length, were used. The heat treatment of the vermicular graphite cast iron consisted of both the austenitization and the austempering processes held at the temperature values of  $T_\gamma$  and  $T_{pi}$ , respectively, the parameters being changed according to the plan. A schematic diagram of the applied heat treatment is shown in Fig. 2. Both the temperature values and duration of each stage of treatment were selected after careful analysis of some studies on heat treatment of nodular and vermicular graphite cast iron [30-37]. The following variants were finally assumed:

- Variant no. 1:  $T_\gamma = 960^\circ\text{C}$ ;  $T_{pi} = 390^\circ\text{C}$ ;
- Variant no. 2:  $T_\gamma = 960^\circ\text{C}$ ;  $T_{pi} = 290^\circ\text{C}$ ;
- Variant no. 3:  $T_\gamma = 900^\circ\text{C}$ ;  $T_{pi} = 390^\circ\text{C}$ ;
- Variant no. 4:  $T_\gamma = 900^\circ\text{C}$ ;  $T_{pi} = 290^\circ\text{C}$ .

The  $100^\circ\text{C}$  difference in the austempering temperature values was assumed in order to obtain structures with various proportions between ferrite and austenite. Both the austenitization and the austempering times were equal to 1.5 hours.

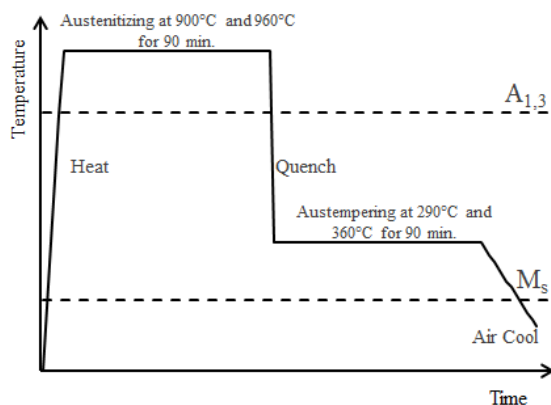


Fig. 2. Schematic diagram of the applied heat treatment

### 3. The results

Figures 3-6 show the microstructure of vermicular graphite cast iron after heat treatment according to the mentioned variants.

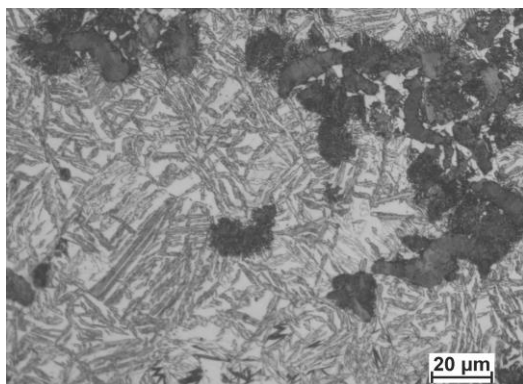


Fig. 3. The microstructure of vermicular graphite cast iron after heat treatment according to variant no. 1 ( $T_{\gamma}=960^{\circ}\text{C}$ ,  $T_{pi}=390^{\circ}\text{C}$ )

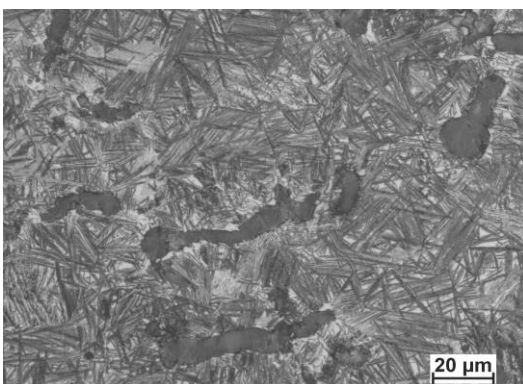


Fig. 4. The microstructure of vermicular graphite cast iron after heat treatment according to variant no. 2 ( $T_{\gamma}=960^{\circ}\text{C}$ ,  $T_{pi}=290^{\circ}\text{C}$ )

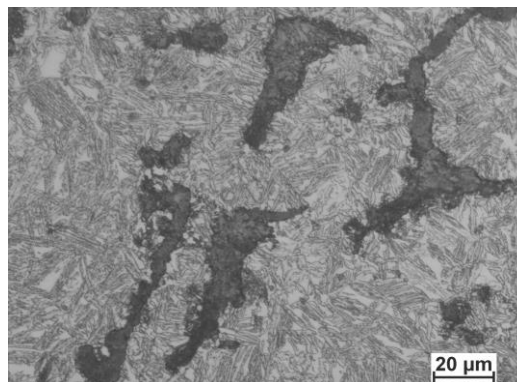


Fig. 5. The microstructure of vermicular graphite cast iron after heat treatment according to variant no. 3 ( $T_{\gamma}=900^{\circ}\text{C}$ ,  $T_{pi}=390^{\circ}\text{C}$ )

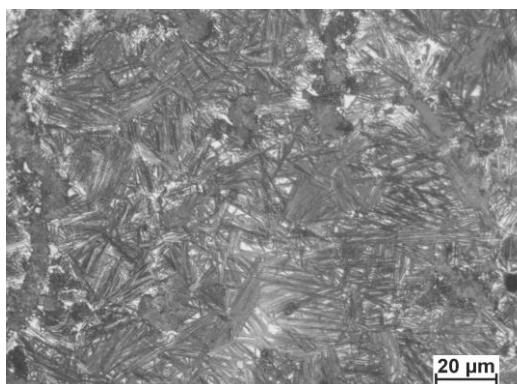


Fig. 6. The microstructure of vermicular graphite cast iron after heat treatment according to variant no. 4 ( $T_{\gamma}=900^{\circ}\text{C}$ ,  $T_{pi}=290^{\circ}\text{C}$ )

In order to determine the fraction of residual austenite, the matrix was analyzed by means of the optical microscope (magn. 400 $\times$ ) at 72 measurement sites. It was found that the examined cast iron types were characterized by the following percentage of austenite:

- in the case of variant 1 - 38.2%;
- in the case of variant 2 - 23.8%;
- in the case of variant 3 - 31.9%;
- in the case of variant 4 - 21.9%.

The ZWICK 1488 testing machine was used to assess the strength properties (according to the PN-EN ISO 527-1). The hardness of the material was evaluated using a Brinell hardness tester equipped with a ball of 2.5 mm diameter applying a load of 1839 N (according to the PN-EN ISO 6506 -1). Average values of the obtained results are presented in Table 2.

The data collected in Table 2 show that the highest values of the tensile strength and the yield point are found for vermicular graphite cast iron subject to the heat treatment according to either variant 2 or variant 4. The lower temperature of austempering (i.e. 290 $^{\circ}\text{C}$ , as opposite to that of 390 $^{\circ}\text{C}$ ) leads to the increase in both the tensile and the yield strength. It is worth noting that the austenitizing temperature influenced the values of  $R_m$  and  $R_{0.2}$ . Higher austenitization temperature (i.e. 960 $^{\circ}\text{C}$ ) causes a decrease in tensile strength by approximately 13%.

An increase in the austempering temperature  $T_{pi}$  from 290°C to 390°C leads to a distinct increase in the unit elongation.

Table 2.

Average values of tensile strength  $R_m$ , elongation  $A_5$ , yield strength  $R_{0.2}$  and hardness HB of vermicular graphite cast iron before and after heat treatment

Specimen type	$R_m$ [MPa]	$R_{0.2}$ [MPa]	$A_5$ [%]	Hardness [HB]
As-cast	371	331	2.1	183
Heat-treated acc. to variant	1	623	1.6	260
	2	824	0.7	334
	3	616	1.0	280
	4	954	0.4	352

The tribological tests were carried out by means of the T-01M tribometer operating in the pin-on-disc system [38]. The tests were carried out in accordance with the ASTM G99 standard.

The cylindrical specimens (pins) for tribological tests had a diameter of 4 mm and a length of about 35 mm. They were cut out of the from the tab ends of tensile specimens. The counter-samples in the form of discs were made of JT6500 friction material based on resins and synthetic rubber with metal and mineral fillers [39]. They had a diameter of 45 mm and a thickness of 5 mm. The specimens were abraded under the conditions of dry friction over a sliding distance of 4000 m. Both the specimen and the counter-sample losses were determined by weighing them every 500 m by means of the WA35 analogue scale, type PRL TA14. A vertically mounted cast iron pin was pressed against the counter-sample with a force of 29.43 N. The abraded surface of a pin was equal to 12.56 mm<sup>2</sup>, and the unit pressure was 2.34 MPa. The sliding speed was 0.55 m/s. The average coefficient of friction for the as-cast material was equal to about 0.35, while for the heat-treated specimens it was about 0.32. The temperature generated at the interface of friction pairs in the final phase of the experiment ranged from 58°C to 64°C.

Figure 7 presents the average results of tribological wear tests carried on for specimens made of vermicular graphite cast iron. Figure 8 shows the mass losses of counter-samples cooperating with the tested cast iron types.

The greatest total mass loss of a specimen over the sliding distance of 4000 m was found for the as-cast material (approximately 6.26 mg); and the lowest mass losses were recorded for the vermicular graphite cast iron austempered at 290°C, i.e. heat-treated according to either variant 2 or variant 4, for which the temperature of austenitization was 960°C or 900°C, respectively, while the recorded mass losses were equal to about 1.0 mg or about 0.8 mg, respectively.

As far as the wear of counter-samples is considered, the greatest mass losses were exhibited by the discs cooperating with the specimens made of the vermicular graphite cast iron heat-treated according to either variant 2 or variant 3, and they were equal to either about 170 mg or about 117 mg, respectively. The lowest mass loss occurred for the counter-sample working with

the material in the as-cast state (approx. 38 mg), the second one with respect to the magnitude of mass loss was the disc cooperating with the specimen heat-treated according to variant 1 (approx. 79 mg).

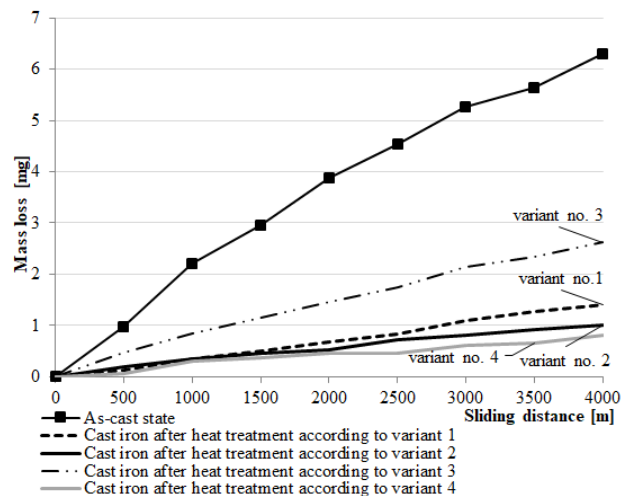


Fig. 7. Average weight losses of vermicular cast iron specimens in the as-cast state and after heat treatment versus the sliding distance

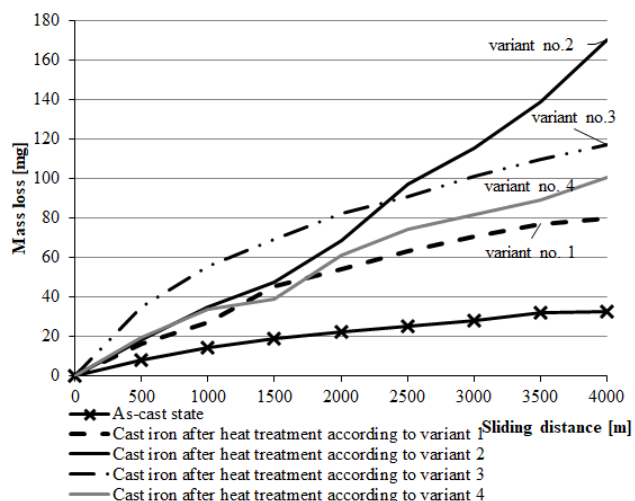


Fig. 8. Average weight losses of counter-samples made of JT6500 friction material versus the sliding distance

Figures 9-11 show the scanned microstructures of the surfaces of the investigated types of cast iron after the abrasion test. The Vega 3 scanning microscope (Tescan) was used for evaluation. One can notice irregular, large grooves and distinct oriented abrasion traces in the photographs. Plastic flow of the material can be recognized on the surface of each specimen. Microcracks and pits generated by tearing out of the material can also be identified. The as-cast material is characterised by local areas of different hardness revealed by the different degrees of tribological wear. One can see that the vermicular graphite cast

iron heat-treated according to variant 3 exhibits particularly deep and wide traces of abrasion.

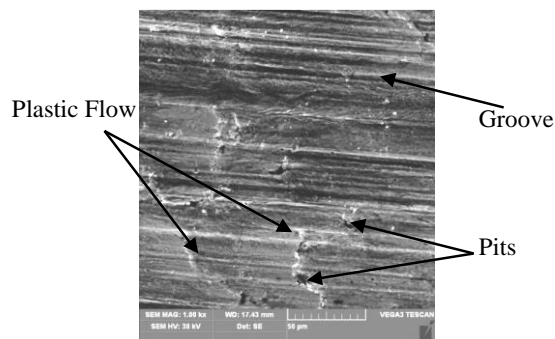


Fig. 9. The surface of the vermicular graphite cast iron in the as-cast state after abrasion; magnification 1000×

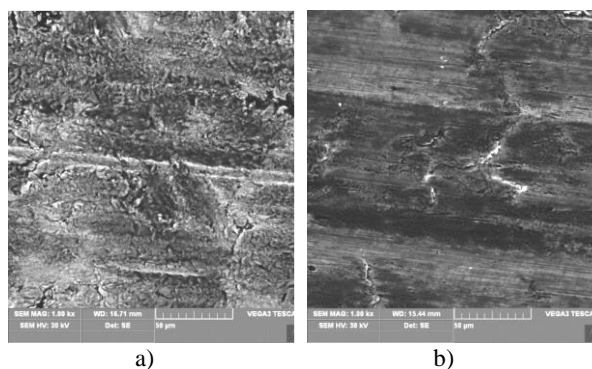


Fig. 10. The surface of the AVGI cast iron after abrasion: a) the alloy heat-treated according to variant 1; b) the alloy heat-treated according to variant 2; magnification 1000×

The abrasive wear tests were extended by the measurement of the roughness of the abraded surfaces of the vermicular graphite cast iron specimens, both those made of the as-cast material, and the heat-treated ones. Measurements were carried out by the contact method using the Taylor Hobson profilometer. The profilometer allows for recording signals coming from the stylus moving along the measured surface in the form of a profilograph. Measurements were taken over the evaluation length of 2.1 mm, while the sampling length of 0.25 mm was chosen. Three measurements were taken for each specimen. Table 3 presents the selected roughness parameters.

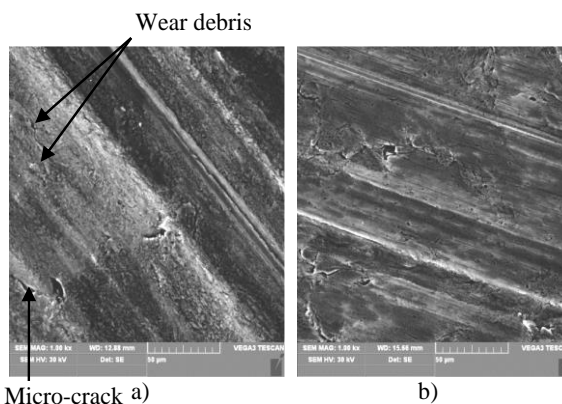


Fig. 11. The surface of the AVGI cast iron after abrasion: a) the alloy heat-treated according to variant 3; b) the alloy heat-treated according to variant 4; magnification 1000×

The obtained data show that the vermicular graphite cast iron subject to heat treatment according to variant 3 is characterized by the highest roughness, the  $R_z$  parameter being 5.61  $\mu\text{m}$ . The  $R_{sm}$  parameter, which determines the mean groove spacing is also the largest one and amounts to approx. 147  $\mu\text{m}$ . Taking the value of the profile height ( $R_z$ ) for the specimen made of the as-cast material as a reference, one can notice that the profile height increased by approx. 40% in the case of the specimen being heat-treated according to the variant 3, while it decreased by about 37% in the case of specimen being heat-treated according to the variant 2.

Table 3.

Average values of roughness parameters for the profiles of vermicular graphite cast iron specimens, both with and without heat treatment, after the abrasion test

Roughness parameters [ $\mu\text{m}$ ]	Specimen type				
	As-cast	Heat-treated according to variant:			
		1	2	3	4
$R_t^{1)}$	5.90	4.11	4.08	7.55	5.15
$R_z^{2)}$	3.99	2.74	2.50	5.61	2.66
$R_a^{3)}$	0.65	0.49	0.46	1.39	0.52
$R_q^{4)}$	0.84	0.64	0.58	1.63	0.71
$R_{sm}^{5)}$	55.9	85.7	101.6	146.6	108.5

<sup>1)</sup> total profile height (between the top of the highest peak and the lowest pit),

<sup>2)</sup> mean roughness depth (average sum of the maximum height of the peaks and the maximum depth of pits within five sampling lengths),

<sup>3)</sup> arithmetic mean of profile ordinates,

<sup>4)</sup> mean square deviation of the profile,

<sup>5)</sup> mean groove spacing along the profile.

## 4. Summary

Five types of vermicular graphite cast iron were examined with respect to their tribological properties within the scope of the research. The abrasion tests were performed both for the initial as-cast material exhibiting a pearlitic-ferritic structure and for four AVGI cast iron types obtained from the initial material by heat treatment according to four variants, which resulted in diversified austenitic-ferritic structures.

The consequent differences in mechanical properties of the AVGI cast iron types (see data in Table 2) are related to the percentage of both ferrite and austenite in the cast iron matrices. For the reduced temperature of austempering, the increased percentage of ferrite in the matrix was observed, and the austenite percentage decreased. The increased percentage of ferrite in the ausferritic matrix subsequently results in the improved plastic properties of the material due to the high plasticity of ferrite, but it happens at the expense of the tensile strength of the alloy.

The formation of ausferrite significantly influences the abrasive wear of the considered cast iron types. The specimens containing about 22% of residual austenite (variants 2 and 4) were characterized by the lowest wear over the sliding distance of 4000 m (1.0 mg and 0.8 mg, accordingly) and by the smallest surface roughness (2.5  $\mu\text{m}$  and 2.66  $\mu\text{m}$ , respectively). It should be noted that the heat treatment according to variant 1 ( $T_{\gamma}=960^{\circ}\text{C}$ ,  $T_{\text{pi}}=390^{\circ}\text{C}$ ) also resulted in satisfactory results: the total wear of the AVGI cast iron obtained after the heat treatment according to variant 1 was only 1.41 mg and the value of surface roughness was equal to 2.74  $\mu\text{m}$ . It can also be seen that the mass loss of all three above mentioned cast iron types (heat-treated according to variant 1, 2, or 4) changed in a very similar way over the sliding distance up to 1500 m.

In the case of counter-sample wear, the lowest wear was found for the disc cooperating with the initial as-cast material of the ferritic-pearlitic structure. The counter-sample wear was also quite low in the case of cooperation with AVGI cast iron after the heat treatment according to variant 1, for which the fraction of residual austenite was equal to approximately 38%.

To summarise, it is worth noting that the heat treatment of the vermicular cast iron influenced both the abrasive wear and the surface roughness of the materials in question. Further analysis would be necessary to find out whether the frictional wear causes changes in the microstructure of the abraded material and what range of operating temperature should be recommended for the AVGI cast iron to ensure its work without a detriment of its microstructure.

## References

- [1] Hebda, M., Wachal, A. (1980). *Tribology*. Warsaw: Ed. Scientific and Technical Publishers.
- [2] Hebda, M. (2007). *Processes of friction, lubrication and wear of machines*. Warsaw – Radom: Ed. Institute of Sustainable Technologies - PIB.
- [3] Podrzucki, C. (1991). *Cast iron. Structure, properties, application*. vol. 1 and 2. Krakow: Ed. ZG STOP. (in Polish).
- [4] Kopyciński, D., Kawalec, M., et al. (2013). Analysis of the structure and abrasive wear resistance of white cast iron with precipitates of carbides. *Archives of Metallurgy and Materials*. 58(3), 973-976.
- [5] Szajnar, J., Walasek, A. & Baron, C. (2013). Tribological and corrosive properties of the parts of machines with surface alloy layer. *Archives of Metallurgy and Materials*. 58(3), 931-936.
- [6] Kovac, P., Jesic, D., Sovilj-Nikic, S., et al. (2018). Energy aspects of tribological behaviour of nodular cast iron. *Journal of Environmental Protection and Ecology*. 19(1), 163-172.
- [7] Cabanne, P., Forrest, R., Roedter, H. (2006). *Sorelmetal about nodular cast iron*. Warsaw: Metals & Minerals Ltd.
- [8] Gumienny, G. (2013). Effect of carbides and matrix type on wear resistance of nodular cast iron. *Archives of Foundry Engineering*. 13(3), 25-29.
- [9] Jeyaprakash, N., Sivasankaran, S., Prabu G., Yang, Che-Hua, & Alaboodi Abdulaziz S. (2019). Enhancing the tribological properties of nodular cast iron using multi wall carbon nanotubes (MWCNTs) as lubricant additives. *Materials Research Express*. 6(4). DOI: <https://doi.org/10.1088/2053-1591/aafce9>
- [10] Wojciechowski A., Sobczak J. (2001) *Composite brake discs for road vehicles*. Warsaw: Motor Transport Institute.
- [11] Guzik, E. (2001). *Cast iron refining processes*. Selected Issues. Archive of Foundry. Monograph No. 1M, 2001. Ed. PAN.
- [12] Duenas, J.R., Hormaza, W. & CastroGüiza, G.M. (2019). Abrasion resistance and toughness of a ductile iron produced by two molding processes with a short austempering. *Journal of Materials Research and Technology*. 8(3), 2605-2612.
- [13] Han, J.M., Zou, Q., Barber, G.C. & et al. (2012). Study of the effects of austempering temperature and time on scuffing behavior of austempered Ni–Mo–Cu ductile iron. *Wear*. 290-291, 99-105
- [14] Du, Y., Gao, X., Wang, X. & et al. (2020). Tribological behavior of austempered ductile iron (ADI) obtained at different austempering temperatures. *Wear*. 456-457(203396), 1-12. DOI: 10.1016/j.wear.2020.203396
- [15] Kocharński, A., Krzyńska, A., Chmielewski, T. & Stoliński, A. (2015). Comparison of austempered ductile iron and manganese steel wearability. *Archives of Foundry Engineering*. 15(spec.1), 51-54.
- [16] Myszka, D. (2005). Microstructure and surface properties of ADI cast iron. *Archives of Foundry*. 5(15), 278-283.
- [17] Kumari, R., Rao, P. (2009). Study of wear behaviour of austempered ductile iron. *Journal of Materials Research*. 44, 1082-1093.
- [18] Medyński, D. & Janus, A. (2018). Abrasive – wear resistance of austenitic cast iron. *Archives of Foundry Engineering*. 18(3), 43-48.
- [19] Pytel, A. & Gazda, A. (2014). Evaluation of selected properties in austempered vermicular cast iron (AVCI). *Works of the Foundry Research Institute*. LIV(4), 23-31.
- [20] Panneerselvama, S., Martis, C.J., Putatunda, S. K. & Boileau, J. M. (2015). An investigation on the stability of austenite in Austempered Ductile Cast Iron (ADI). *Materials Science and Engineering: A*. 625, 237-246.

- [21] Kim, Y., Shin, H., Park, H. & Lim, J. (2008). Investigation into mechanical properties of austempered ductile cast iron (ADI) in accordance with austempering temperature. *Materials Letters*. 62(3), 357-360.
- [22] Krzyńska, A. (2013). Searching for better properties of ADI. *Archives of Foundry Engineering*. 13(spec.1), 91-96.
- [23] Krzyńska, A. & Kočański, A. (2014). Austenitization of Ferritic Ductil Iron. *Archives of Foundry Engineering*. 14(4), 49-54.
- [24] Wilk-Kołodziejczyk, D., Mrzygłód, B., Regulski, K. & et al. (2016). Influence of process parameters on the properties of austempered ductile iron (ADI) examined with the use of data mining methods. *Metallurgija*. 55(4), 849-851.
- [25] Khalaj, G., Pouraliakbar, H., Mamaghaniz, K. R. & et al. (2013). Modeling the correlation between heat treatment, chemical composition and bainite fraction of pipeline steels by means of artificial neural networks. *Neural Network World*. 23, 351-367.
- [26] Kiahosseini, S. R., Baygi, S., J., M., Khalaj, G. & et al. (2017). a study on structural, corrosion, and sensitization behavior of ultrafine and coarse grain 316 stainless steel processed by multiaxial forging and heat treatment. *Journal of Materials Engineering and Performance*. 27, 271-281.
- [27] Polish Standard PN-EN 1563, Founding. Spheroidal graphite cast iron, (2000).
- [28] Polish Standard PN-EN ISO 945-1: Microstructure of cast irons. Part 1. Graphite classification by visual analysis. November 2009. Correction PN-EN ISO 945-1:2009/AC. April 2010.
- [29] Polish Standard PN-75/H-04661: Grey cast iron, nodular cast iron and malleable. Metallographic examinations. Determining of microstructure.
- [30] Soński, M.S., Jakubus, A. (2014). Initial assessment of abrasive wear resistance of austempered cast iron with vermicular graphite. *Archives of Metallurgy and Materials*. 59(3), 1073-1076.
- [31] Kaczorowski, M. (2001). Structure and mechanical properties of ADI cast iron. *Archive of Foundry*. 1(1/2), 149-158.
- [32] Myszka, D., Kaczorowski, M., Tybulczuk, J. & Kowalski, A. (2004). Parameters of the ADI cast iron production process and its mechanical properties. *Archive of Foundry*. 4(11), 355-364.
- [33] Binczyk F., Gradoń P. (2010). *Influence of heat treatment parameters on the formation of ADI cast iron microstructure*. The work of IMŻ. 4, 5-14.
- [34] Pietrowski, S. (1997). Ductile iron with the structure of bainitic ferrite with austenite or bainitic ferrite. *Archives of Materials Science*. 18, 253-273.
- [35] Borowski, A.W. (1998). Synthetic ductile iron quenched with isothermal transformation (ADI). XXIII Scientific and Technical Symposium of the Foundry Engineering ITMat. Warsaw University of Technology, pp. 29.
- [36] Wróbel, J. (2013). *Cast iron thermal fatigue resistance ADI*. Crakow: PhD thesis. AGH.
- [37] Mierzwa, P. (2010). The effect of thermal treatment on the selected properties of cast iron with vermicular graphite. Doctoral thesis. Czestochowa University of Technology.
- [38] Institute of Sustainable Technologies. User manual. Tribology set T -01M, mandrel-disc type. State Research Institute. Radom 2010.
- [39] makland.com.pl. 28.02.2016, time 13.25.